

Sub-exemplar Shape Tuning in Human Face-Related Areas

Sharon Gilaie-Dotan and Rafael Malach

Department of Neurobiology, Weizmann Institute of Science, Rehovot 76100, Israel

Although human face recognition performance shows high selectivity, even for unfamiliar faces, the neuronal circuitry underlying this high performance is poorly understood. Two extreme alternatives can be considered: either a “labeled-line” principle, in which subtle changes in face images lead to activation of differently tuned neuronal populations, or a coarse coding principle, where the high face selectivity is coded by the relative activation of broadly tuned neurons. In this study, we set to parametrically examine the shape and selectivity profile of face-related visual areas. To that end, we applied the functional magnetic resonance (fMR)-adaptation paradigm. Unfamiliar face stimuli were morphed into sets ranging from identical faces, through subtle morphing, to completely different exemplars. The fusiform face area (FFA) revealed high face sensitivity, so that even facial images perceived as belonging to the same individual (<35%) were sufficient to produce full recovery from adaptation. Interestingly, the psychophysical detectability of facial differences paralleled the release from fMR-adaptation. These results support the labeled-line model where high sensitivity to face changes is paralleled by narrow tuning of neuronal populations selective to each face image, and they suggest that fMR-adaptation is closely related to behavior. The results bear strong implications to the nature of face-related neuronal responses.

Keywords: faces, FFA, fMR-adaptation, fMRI, vision

Introduction

A significant specialization of human perceptual capabilities is its exquisite sensitivity to faces. Beyond the ability to identify familiar faces, despite many facial changes (aging-induced changes, expressions, hairstyles, etc.), people can detect and distinguish an unfamiliar face image even from very similar face distracters well above chance (Bruce and others 1991; Hancock and others 2000; Le Grand and others 2004). How is such a remarkable performance accomplished at the neuronal representation level? Basically, one can envision a spectrum of possibilities bracketed by 2 extreme models. One possibility, whose paradigmatic example is the sound frequency coding of the auditory nerve fibers, is a labeled-line model, in which neurons are narrowly tuned, so that slight changes in a face image will result in a shift of the activity from one set of neurons to a completely different set (Fig. 1A, left). The other extreme possibility—exemplified by color coding in the retina—is a distributed coding representation, in which individual neurons are broadly tuned and may respond to large variations in faces, but the sensitivity to each face is expressed through the relative levels of activation within the neuronal representation (Fig. 1A, right).

Recent neuroimaging studies have uncovered a clear selectivity to faces within the high-order occipitotemporal areas

in the human visual cortex (Kanwisher and others 1997; Halgren and others 1999; Ishai and others 1999; Hasson and others 2001, 2004). Using a wide array of stimuli, it has been shown that a consistent feature of these areas is a preferential activation to face images compared with other object categories, although the exact role of such selectivity is still debated (Kanwisher and others 1997; Gauthier and others 2000; Haxby and others 2001; Levy and others 2001; Spiridon and Kanwisher 2002).

Concerning the nature of the face representation, several studies indicate that when examining the global functional magnetic resonance imaging (fMRI) signal within the most selective face-related area (found in the posterior fusiform gyrus, known as the fusiform face area [FFA] [Kanwisher and others 1997]), the apparent tuning is rather broad. An illustration of this effect was reported when examining the activation levels of this area to a wide variety of subcategories of faces: the response is of similar magnitude to front view, profile view, 2-tone “Mooney” faces, cat faces, and cartoon faces (Kanwisher and others 1998; Tong and others 2000). A recent study (Pourtois and others 2005) using an event-related paradigm found no significant differences between the average activation to front views and 3/4 views in face-selective areas in the fusiform cortex. Even more surprising is the finding that this area shows only a mild effect of difference in the average fMRI signal between inverted faces and upright faces (Kanwisher and others 1998).

One might conclude from these results that the shape tuning of visual activation of neuronal populations in the FFA face-selective area is very broad—that is, that the neural machinery is very tolerant to shape changes.

However, as we have argued previously (Grill-Spector and others 1999), measuring the averaged neuronal activity within a voxel might mask a more finely organized heterogeneous population of neurons, providing the apparent impression of a nonselective behavior (Beauchamp and others 2004). More specifically to the issue of face selectivity, an imaged voxel might show broadly tuned face response in the fMRI signal, although it is actually composed of a heterogeneous populations of neurons that are individually narrowly tuned to specific face images. Such broad tuning in the fMRI signal can emerge if a voxel comprises roughly balanced populations of neurons, which are each highly selective to different individual faces, so that the activity of these individually selective populations are averaged together into an apparently broadly tuned fMRI signal.

One way we have proposed to circumvent this problem is through functional magnetic resonance (fMR)-adaptation (Grill-Spector and Malach 2001). Basically, the approach takes advantage of the finding that repeated presentation of the

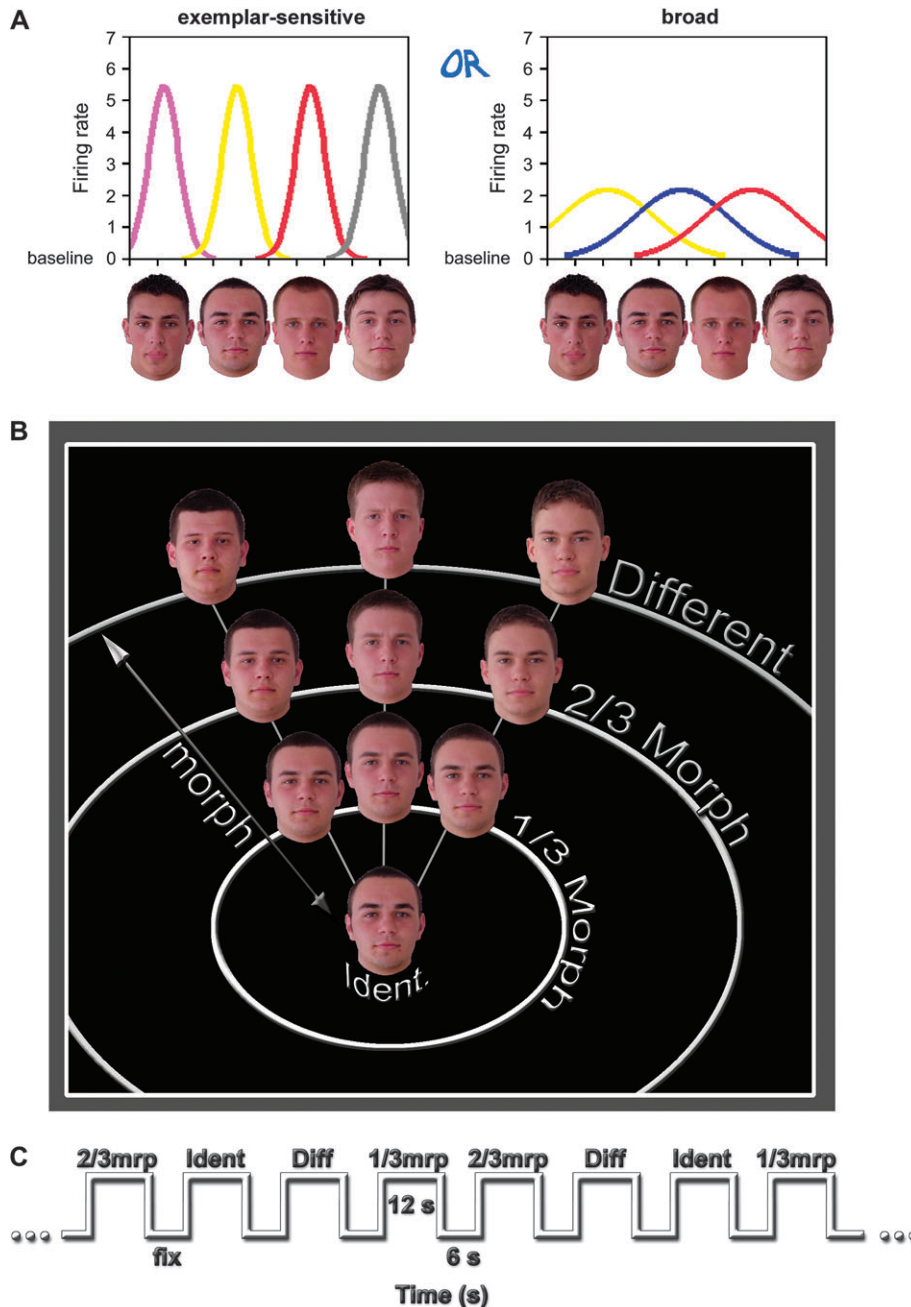


Figure 1. Face representations: models and experimental design. (A) Two possible alternatives for how neurons represent faces in face-selective regions. Left—exemplar-sensitive model where each neuron is narrowly tuned to a specific face image. Right—broadly tuned model where the face representation is based on the relative activity among the broadly tuned channels. (B) Face space rendition of the 4 conditions in the block design experiment. A face (identical) was gradually morphed to various different faces (different), and the faces at 2 intermediate points along the morph (1/3 and 2/3 of the way) were taken as “1/3 morph” and “2/3 morph” conditions. Note the perceptual similarity among the different faces at the 1/3 morph level. (C) A segment from the time axis of the experiment that lasted 480 s. The experiment consisted of 24 visual blocks of 12 s each. Each condition was repeated 6 times with different face images, as described in (B).

same stimulus leads to reduced activation of the responsive neurons. By manipulating the parameter of interest of the stimulus and by measuring the extent to which the neuronal population is released from the adaptation, one can obtain an indirect measure of the sensitivity of the activated neuronal population to this parameter (Tootell and others 1995; Kourtzi and Kanwisher 2001; Huk and Heeger 2002; Kourtzi and others 2003). Pourtois and others (2005) have investigated the sensitivity to viewpoints (front vs. 3/4 view) of the same face in face-selective regions, using this approach. They found that

for unfamiliar faces the cortical representations are viewpoint sensitive. Recently, Rotshtein and others (2004) have applied this approach to examine face tuning across identities (exemplars) with famous faces in high-order face areas. They compared the adaptation level in face-related areas to repeated presentations of the same face image with the adaptation levels to pairs of morphed famous faces along the morph continuum. Their results revealed a tuning that was linked to the perceptual “identity boundary” or “category boundary” that occurs behaviorally at 50% morph distance from the original face (Beale and

Keil 1995; Campanella and others 2000). We will refer to this perceptual boundary (50% morph) as the perceptual differentiation between exemplars (“exemplar boundary”), and by sub-exemplar, we will refer to morph levels that are still behaviorally classified as same exemplar (<50% morph). Rotshtein and others found no sensitivity of the tuning for sub-exemplars (no release from adaptation) and sensitivity only when crossing the perceptual exemplar boundary (between identities). However, it could be argued that such a sensitivity in the tuning, which is linked to the exemplar boundary, might be due to prior exposure to the famous faces. Here we applied parametrical morph to unfamiliar faces, where no such preexposure was possible. Our results show that for unfamiliar faces, FFA shows notable sub-exemplar sensitivity—when examined through fMR-adaptation. Some of these results have been presented in abstract form (Gilaie-Dotan and Malach 2004).

Methods

Subjects

Altogether, 25 healthy different subjects participated in the fMRI (block design and rapid event-related design) and the behavioral experiment. Twelve subjects (7 women, aged 22–53) participated in the block design experiment. Eight subjects (5 women, aged 22–32) participated in the rapid event-related experiment and 7 subjects (4 women) in the behavioral experiment. All subjects participating in the fMRI experiments underwent a short training session of 2 min prior to the scan on a different set of stimuli. All subjects had normal or corrected-to-normal vision. All the fMRI subjects provided written informed consent to participate in the experiments. The Tel Aviv Sourasky Medical Center approved the experimental protocol.

Magnetic Resonance Imaging Setup

Subjects were scanned in a 1.5-T Signa Horizon LX 8.25 GE scanner equipped with a standard head coil. Blood oxygenation level-dependent (BOLD) contrast was obtained with gradient-echo echo planar imaging (EPI) sequence. The block-design experiment time repetition (TR) = 3000 ms, echo time (TE) = 55 ms, flip angle = 90°, field of view = 24 × 24 cm², matrix size = 80 × 80, the scanned volume consisted of 24–26 nearly axial slices of 4-mm thickness and 1-mm gap with an in-plane resolution of 3 × 3 mm², covering the entire cortex. The rapid event-related experiment TR = 1500 ms, TE = 55 ms, flip angle = 70°, field of view 24 × 24 cm², matrix size 80 × 80, the scanned volume consisted of 13 oblique slices of 4-mm thickness and 1-mm gap with an in-plane resolution of 3 × 3 mm² in order to cover completely the occipital and temporal lobes and reaching up to the ventral aspect of the parietal lobe.

A whole-brain spoiled gradient (SPGR) sequence was acquired on each subject to allow accurate cortical segmentation, reconstruction, and volume-based statistical analysis. T₁-weighted high-resolution (1.1 × 1.1 mm²) anatomic images of the same orientation as the EPI slices were also acquired to facilitate the incorporation of the functional data into the 3-dimensional (3D) Talairach space (Talairach and Tournoux 1988).

Button presses were recorded during the fMRI experiments via a response box from which we analyzed the behavior performance (reaction time [RT] and percent correct).

Stimuli

Stimuli were generated on a PC, projected via an LCD projector (Epson MP 7200) onto a tangent screen positioned over the subject’s forehead, and viewed through a tilted mirror. Stimuli were based on 78 original different color photographs of male faces taken from 2 databases (mainly CVL Face Database [http://www.lrv.fri.uni-lj.si/facedb.html] and also AR Face Database [Martinez and Benavente 1998]). Frontal images were chosen of mostly Caucasian, with neutral expression, mouth closed, no facial hair, and no glasses. The original images were then processed using Adobe Photoshop 6 in the following manner:

rotated to upright, such that the line connecting the eyes was horizontal; aligned to each other by rescaling to a common face size and location and then aligned by the middle vertical line crossing the nose of each face and by the horizontal line that passes below the eyes; the background was set to black, and the neck was cropped naturally (as if wearing high-neck black shirt); hairstyle was set above the ears and images were cropped to 300 × 300 pixels (12° × 12°).

The morphing of the original images was done using MorphMan 4.0 (STOIK Imaging, Moscow, Russia). The morphing was done in sets of 13 different original images, where 1 face was morphed to 12 different faces. The main alignment features for the morph included hairline, lips, nose, eyes, eyebrows, and the external contour.

The fixation image was a black image (matching the black background of the face stimuli). A red fixation dot of two-by-two pixels (0.08° × 0.08°) was imposed on all stimuli in the center.

Block Design fMRI Experiment

The experiment lasted 480 s and included 4 conditions: identical, 1/3 morph, 2/3 morph, and different. Each condition was repeated 6 times in a controlled and counterbalanced block design paradigm. Each block lasted 12 s, with interleaving 6-s fixations between blocks. The first and last fixations lasted 21 and 15 s, respectively. A block consisted of 12 different stimuli; each stimulus was presented for 1000 ms. Consecutive images were slightly shifted in an equally balanced manner (across conditions, across Euclidean distance) in all conditions to avoid motion cue confounds and to eliminate tactics of retinal differences. All 11 translations within a block were equal in size, following a translation path along 12 symmetrical points (with regard to the *x* axis and *y* axis) in a 2D square (maximum size 0.68° × 0.68°). Average translation between 2 consecutive images over all translations in the experiment was 0.29° (minimum 0.18°, maximum 0.38°). The average Euclidean distance of the shifted images, which were controlled for Euclidean distance (with a minimal Euclidean distance being the average distance of the 2/3 morph condition, which is perceptually equivalent to the different condition), was as follows—identical: 23.60, 1/3 morph: 22.80, 2/3 morph: 21.54, and different: 26.23. Average Euclidean distance in a block across the whole experiment was 23.49 (see details below). Subjects’ task was to fixate and respond via a response box whether a face image was the same face image (should report “same”) or a different face image (should report “different”) than the previous one.

To allow for a 1-back recognition task, in the identical condition, we introduced occasionally a matching 1/3 morph image (of the 6 identical blocks, 2 blocks contained no 1/3 morph image, 2 blocks contained one 1/3 morph image [derived from the block’s identical face], and 2 blocks contained two 1/3 morph images), whereas in the other conditions, occasional repetitions were inserted (in each of the 1/3 morph, 2/3 morph, and different conditions, of the 6 blocks per condition, 2 contained no repetitions, 2 contained 1 repetition, and 2 blocks contained 2 repetitions).

The experiment was run in 2 versions (counterbalanced across subjects). The difference between the versions was that in each version the base face for the morph of each set was a different face (out of the same 13 faces that composed the set). See Stimuli subsection for further details. Each version consisted of 222 different male facial images made of 78 (6_{rings} × 13_{images per ring}) different original faces (of different men) and 144 (6 × 12 × 2) morphed images. Only the morphed images were different between the 2 versions.

Euclidean Distance

For each pair of images (*K*, *J*) in a block, for each color channel (R, G, B) separately, Euclidean distance was defined by $d(K, J) = 1/\sqrt{\text{imgsize}} \sqrt{\sum (K - J)^2}$ with *K*, *J* measured in (0,255) units. The block distance for each channel was defined as the average distance across all pairs (*K*, *J*) in the block. The average Euclidean distance was defined as the average distance over all blocks and all the 3 RGB channels.

Rapid Event-Related fMRI Experiment

Two scans of 2 versions were run on each subject (version order counterbalanced across subjects). Each version lasted 423 s. The

experiment employed a rapid event-related paradigm with 4 main conditions: 40% morph, 30% morph, 10% morph, identical, and a fixation condition, ordered in a counterbalanced manner. Each condition was repeated 50 times across the 2 scans. Events lasted 3 s: 1200 ms of fast image presentation (200 ms picture + 100 ms fixation, 4 times) + 1800 ms fixation. Each event consisted of 4 stimuli. On trials with nonidentical stimuli, 4 different images were presented. Subject's task was a same/different task, and they were asked to report different if any change at all was noticed for each brief face presentation or same—only if no change was noticed. The first and last fixations lasted 21 and 15 s, respectively. Each version included 325 ($25_{\text{reps}} \times 4_{\text{images per event}} \times 3_{\text{cond}} + 25_{\text{images per identical}}$) different stimuli.

Behavioral Experiment

This experiment was aimed at defining the profile of difference-perception according to the morph levels (0–45% in 5% steps, and 100%). It also enabled us to decide which conditions will be used in the rapid event-related fMRI experiment. The event-presentation setup was the same as in the rapid event-related fMRI experiment. The experiment included 12 conditions (11 morph levels and fixation), each repeated 12 times in a counterbalanced order. The first and last fixations lasted 2 s each, altogether lasting 436 s.

Mapping Retinotopic Borders of Visual Areas

As described earlier (Levy and others 2004a), the representations of vertical and horizontal visual field meridians were mapped to delineate borders of retinotopic areas (Sereno and others 1995; DeYoe and others 1996; Engel and others 1997) in all the 12 subjects who participated in the block design experiment (data of 1 subject were omitted due to poor fMRI data, and a “house face localizer” experiment [Levy and others 2001] was used to delineate the FFA anatomical location) and in 6 out of the 8 subjects that participated in the event-related experiment. Out of the 6 subjects (event-related experiment) that were included in the FFA right hemisphere analysis, for the 2 that did not have their retinotopic areas mapped, a house face localizer experiment (Levy and others 2001) was used to delineate the FFA anatomical location.

Data Analysis—Block and Event-Related Design Experiments

fMRI data were analyzed with the BrainVoyager software package (R.Goebel, Brain Innovation, Maastricht, The Netherlands) and with complementary in-house software. The first 2 images of each functional scan were discarded. The functional images were superimposed on 2D anatomic images and incorporated into the 3D data sets through trilinear interpolation. The complete data set was transformed into Talairach space (Talairach and Tournoux 1988). Preprocessing of functional scans included 3D motion correction, slice scan time correction, linear trend removal, and filtering out of low frequencies up to 5 cycles per experiment. No spatial smoothing was applied to the data. The cortical surface was reconstructed from the 3D SPGR scan. The procedure included segmentation of the white matter using a grow-region function, the smooth covering of a sphere around the segmented region, and the expansion of the reconstructed white matter into the gray matter. The surface of each hemisphere was then unfolded, cut along the calcarine sulcus and additional predefined anatomical landmarks on the medial side, and flattened.

Statistical Analysis—Block Design Experiment

The statistical analysis was based on the general linear model (Friston and others 1994). A hemodynamic lag of 3 or 6 s was fitted to the model of each subject by maximizing the extent of the overall visual activations. A boxcar predictor was constructed for each experimental condition except fixation, and the model was independently fitted to the signal of each voxel. A coefficient was calculated for each predictor using a least squares algorithm. FFA face-selective regions were defined for each subject separately using the “internal localizer” procedure (Supplementary Fig. 1; see details below) with the different > identical contrast and were defined as clusters of at least 6 contiguous functional voxels with $P < 0.05$, uncorrected, in the posterior fusiform gyrus anterior to retinotopic areas (see Mapping Retinotopic Borders of Visual Areas for more details). For 10 subjects, FFA face-selective regions were identified (7 subjects with both hemispheres, 3 with right hemisphere only) whereas 2 subjects did not show any adaptation with this internal localizer procedure. Additional FFA region of interest (ROI) analysis was based on faces > fixation contrast (at least 6 contiguous functional voxels, $P < 10^{-4}$, uncorrected, beyond retinotopic areas) and was sampled for both hemispheres in 11 subjects (out of the 12, due to noisy retinotopic mapping in 1 subject). Occipital face area (OFA) face-selective voxels were defined by the same statistical criteria (as described above for the FFA by the internal localizer procedure), residing in lateral-occipital (LO) aspect of the cortex in the vicinity of the inferior occipital sulcus or inferior occipital gyrus, respectively. Six subjects exhibited OFA face-selective foci (2 subjects with both hemispheres, 4 with right hemisphere only). See Table 1 for more details concerning the ROIs that participated in the analysis.

Multisubject Analysis—Block Design Experiment

In the multisubject analysis, time courses of all subjects were converted into Talairach space and z-normalized. The multisubject maps (Supplementary Fig. 2A, Fig. 2) were obtained using a random effect (RE) procedure (Friston and others 1999) and the maps were projected on a flattened Talairach normalized brain.

Internal Localizer Procedure—Block Design Experiment

The approach is aimed to examine the behavior of a region, independently of the statistical test that is used to define it (Lerner and others 2002; Hasson and others 2003; Mukamel and others 2005). To that end, each experiment is essentially split into 2 separate time segments: one segment of the data is used to define the ROI and the complementary segment of the data is used to examine the activation profile and to analyze its correlation to behavior. Note that in this approach the activations used for analysis are independent from the ROI definition. More specifically, as illustrated in Supplementary Figure 1, because we wanted to examine voxels that exhibited adaptation, the voxels were chosen by the test different > identical using a subset of 4 (out of 6) repetitions of each condition, and the activation pattern during the 2 remaining repetitions of these conditions was analyzed independently. This procedure was repeated 3 times such that the 2 analyzed repetitions would not overlap across the 3 samplings. For each subject, from each ROI sampling (of the three), the time course from that ROI was analyzed separately, to create an average response profile for the block (epoch) of each condition (conceptually like the ones presented

Table 1
Talairach coordinates of face-selective regions

Region	Experiment	ROI definition	Left				Cluster size	Right				Cluster size
			n	x	y	z		n	x	y	z	
FFA	block	Different > identical ^a	7	-36 ± 1	-54 ± 2	-18 ± 1	277 ± 68	10	29 ± 2	-47 ± 2	-14 ± 1	339 ± 61
		Faces > fixation	11	-34 ± 1	-54 ± 2	-18 ± 1	456 ± 29	11	29 ± 1	-50 ± 2	-17 ± 1	486 ± 34
	Rapid event related	40% morph > identical	5	-31 ± 2	-58 ± 4	-19 ± 2	180 ± 28	6	31 ± 3	-57 ± 3	-15 ± 2	127 ± 18
		Faces > fixation	7	-34 ± 2	-55 ± 2	-19 ± 3	323 ± 117	7	33 ± 2	-55 ± 2	-17 ± 3	321 ± 146
OFA	Block	Different > identical ^a	2	-42 ± 5	-74 ± 1	-8 ± 0	437 ± 23	6	39 ± 2	-64 ± 3	-10 ± 2	388 ± 48
	Rapid event related	40% morph > identical	4	-40 ± 2	-68 ± 2	-11 ± 7	271 ± 136	5	37 ± 2	-69 ± 4	-6 ± 6	313 ± 116

Note: n, number of subjects with activation according to the ROI definition; x, y, z values in millimeters ± standard error of mean (SEM); cluster size in cubic millimeter ± SEM.

^aDifferent > identical contrast via internal localizer procedure (see Methods and Supplementary Fig. 1 for more details).

in Fig. 3C,D, Supplementary Fig. 3B). This was done by first calculating the percent signal change (PSC) for each time point along a block (relative to the preceding fixation block), and then the average response profile of each condition was taken as the average response profile across all the repetitions of the same condition (for the identical and different condition, only the 2 independent repetitions were averaged). Following this, the subject's response profiles in each condition were calculated by averaging the response profiles of each condition from the 3 samplings. Finally, for each condition, the average response profile was calculated as the average across subjects. Note that the same analysis was done to the localizer repetitions and is presented as a reference (Fig. 3C).

Statistical Analysis—Event-Related Experiment

For each subject, after the time courses of the 2 scans were transformed into Talairach space and preprocessed (see Data Analysis), they were z-normalized and concatenated, and the statistical tests were done on the concatenated time course.

The data were then deconvolved using the deconvolution analysis for rapid event-related paradigms, which consists of a general linear model analysis (Friston and others 1994) in BrainVoyager software package (R.Goebel, Brain Innovation), in order to extract the estimated hemodynamic response in each voxel for each condition. The analysis was done separately for each subject on a voxel by voxel basis.

FFA ROI was defined for each subject as clusters in the posterior fusiform gyrus of at least 6 contiguous functional voxels, anterior to

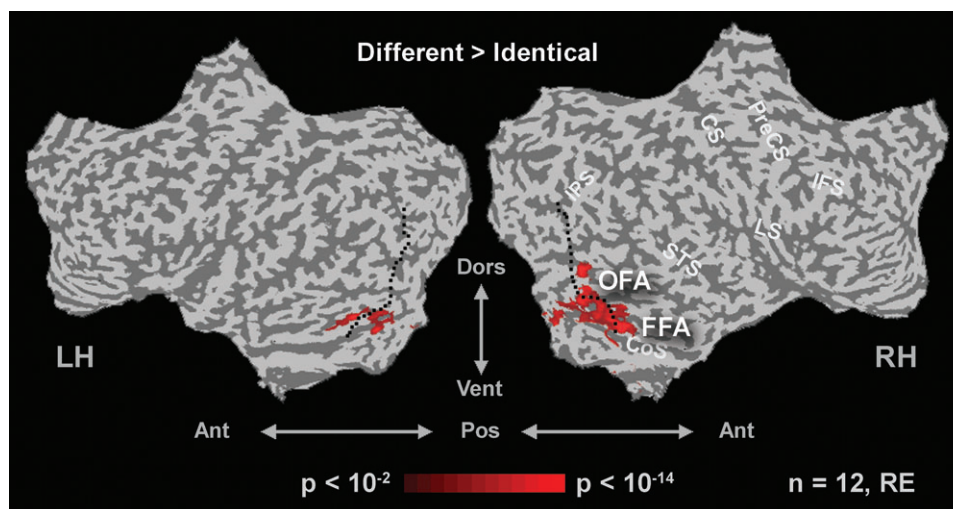


Figure 2. fMRI-Adaptation to face repetition. Unfolded cortical maps showing all the regions that were activated above baseline and showed significantly reduced activation during the identical condition (different > identical contrast). Multisubject analysis, $P < 0.003$, $n = 12$, RE, uncorrected. The black dotted line indicates the estimated anterior retinotopic border of 12 subjects. Note localized adaptation around occipitotemporal cortex. Colors according to significance levels. CoS, collateral sulcus; IPS, intraparietal sulcus; CS, central sulcus; LS, lateral sulcus; IFS, inferior frontal sulcus; Ant, anterior; Pos, posterior; Vent, ventral; Dors, dorsal; LH, left hemisphere; RH, right hemisphere.

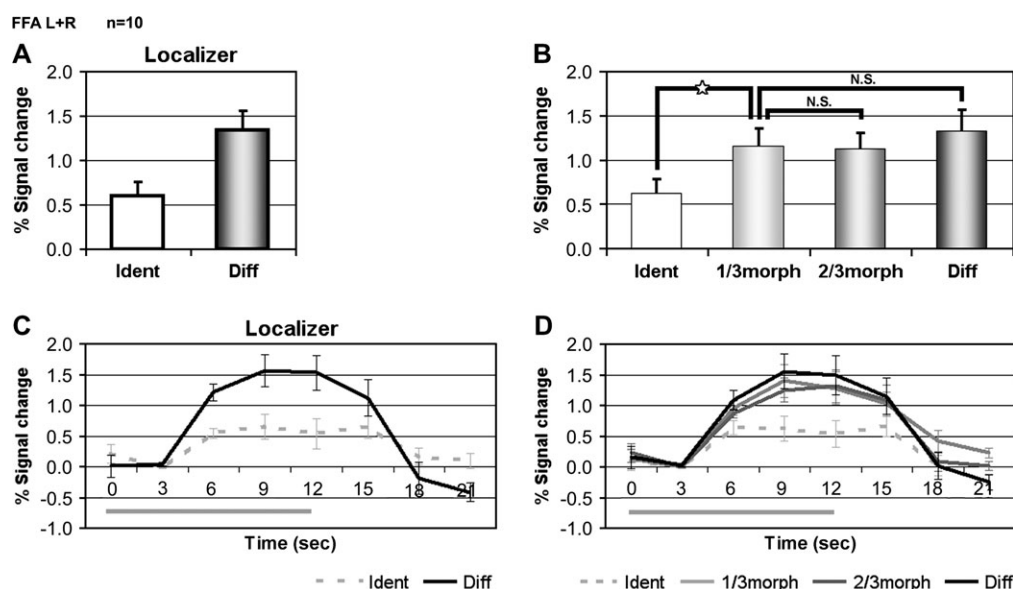


Figure 3. FFA activation during the adaptation experiment (block design). Time course data from 10 subjects. Left (A, C)—statistically biased internal localizer data (see Methods) shown as reference. Right (B, D)—independent blocks, main results. Top (A, B)—average activation levels to the different conditions. Bottom (C, D)—average hemodynamic response for each condition taken from the same voxels as above, measured along time (in seconds, x axis). The gray line below the x axis represents stimulus on. The y axis denotes fMRI BOLD PSC relative to fixation blocks. Asterisk (for the independent data only) denotes a significant difference between identical and 1/3 morph. No significant difference was found between the 1/3 morph and the different or the 2/3 morph condition, indicating a complete recovery from adaptation in the 1/3 morph condition. This indicates high sensitivity of the FFA at the sub-exemplar level and strongly supports the narrow tuning model for the FFA. Error bars, standard error of mean.

retinotopic areas (see Mapping Retinotopic Borders of Visual Areas for more details), with $P < 0.05$ (uncorrected) for the 40% morph $>$ identical contrast (based on all the predictors of these conditions). Additional FFA ROI (analysis provided separately) was defined for each of the 8 subject by faces $>$ fixation contrast, $P < 0.05$, uncorrected, beyond retinotopic areas.

Relating fMRI Results to Behavior

To obtain a quantitative estimate of the release from adaptation and check whether this estimate is correlated to the behavioral measurements, we calculated adaptation recovery measure (Grill-Spector and others 1999, 2000) for each fMRI-measured point along the morph axis (0-1), after block- and event-related data were put on a common baseline, together with behavior. Specifically, because event-related activation levels are considerably smaller than block design activations, we set to calibrate the event-related data onto the block design data (already spanning the [0, 1] morph range) by using 2 common activation points along the morph axis: the identical condition and the 40% morph condition. Because the 40% morph condition did not specifically exist in the block design experiment, we therefore assessed it by calculating the weighted average of the activation levels to the 1/3 morph and 2/3 morph conditions (this was a legitimate calculation because there was no significant difference between the activation levels of these 2 conditions). Because different subjects participated in the block design and event-related experiments, the average activation levels of each of the block design conditions (over all the subjects) were used for the calibration. So for each subject, event-related activations of each condition were calibrated (realigned) into block data scale:

$$(*) \text{signal}(\text{adjusted}) = \overline{\text{ident}_{\text{block}}} + (40\% \text{morph}_{\text{est}} - \overline{\text{ident}_{\text{block}}}) \times \frac{\text{signal} - \text{signal}(\text{ident})}{\text{signal}(40\% \text{morph}) - \text{signal}(\text{ident})},$$

where for each block condition (identical, 1/3 morph, 2/3 morph, different), $\overline{\langle \text{condition} \rangle_{\text{block}}} = \text{mean}_{\text{block-subj}} \{ \text{signal}(\langle \text{condition} \rangle) \}$ and $40\% \text{morph}_{\text{est}} = (4/5)(1/3 \text{morph}_{\text{block}}) + (1/5)(2/3 \text{morph}_{\text{block}})$.

Now, after all the fMRI data (block and event-related) were in the same scale, we calculated the normalized adaptation ratio for each fMRI-measured point along the morph axis by

$$\text{Adaptation-ratio}_{\text{morph-level}}(\text{norm}) = \text{mean}_{\text{subjects}} \left\{ \frac{\text{signal}_{\text{morph-level}} - \text{signal}(\text{ident})}{\text{signal}(\text{diff}) - \text{signal}(\text{ident})} \right\}$$

for block data points (0%, 33%, 67%, and 100% morph), with the adjustment of $\text{signal}(\text{ident}) = \overline{\text{ident}_{\text{block}}}$ and $\text{signal}(\text{diff}) = \overline{\text{diff}_{\text{block}}}$ for the event-related points (10%, 30%, 40%). Note that the $\text{signal}(\text{ident})$ of the block data and event-related data is the same after the calibration.

With respect to the behavioral data, it was rescaled to (0, 1) range as well (fMRI subjects' behavioral data from the 2 experiments were coaligned in the same manner as the fMRI signals):

$$\text{Behavior}_{\text{morph-level}}(\text{norm}) = \text{mean}_{\text{subjects}} \left\{ \frac{\% \text{perceived}(\text{diff})_{\text{morph-level}} - \% \text{perceived}(\text{diff})_{\text{ident}}}{\% \text{perceived}(\text{diff})_{\text{diff}} - \% \text{perceived}(\text{diff})_{\text{ident}}} \right\};$$

$$\text{Behavior}(\text{fMRI})_{\text{morph-level}}(\text{norm}) = \text{mean}_{\text{subjects}} \left\{ \frac{\% \text{perceived}(\text{diff})_{\text{morph-level}} - \% \text{perceived}(\text{diff})_{\text{ident}}}{\% \text{perceived}(\text{diff})_{\text{diff}} - \% \text{perceived}(\text{diff})_{\text{ident}}} \right\};$$

with the same adjustments (calibrations) as in (*) above for the event-related behavior.

Results

Measuring Face Tuning: Block Design

To examine the sensitivity of face-related areas to slight face changes, we examined the adaptation level to parametrically changed morphing levels of unfamiliar faces. Our experimental approach was inspired by the face space concept (Rhodes and

others 1987, 1998; Valentine 1991; Valentine and Endo 1992; O'Toole and others 1997; Leopold and others 2001; Wilson and others 2002). We used a morphing technique to gradually morph one face to other different faces (Fig. 1B). This allowed us to look at sets of faces with growing amounts of facial variability at intermediate points along the morph axis between 0 (being the original face) and 1 (being the different faces).

Figure 1B,C illustrates the basic design of the experiment. The adaptation was measured in the 4 conditions of the experiment (see Methods for details). In the repeat condition (identical), the same face was repeated 12 times in a block. In the different condition, a sequence of 12 different faces was presented during the block. Finally, in the 2 morphed conditions, a single face, which was the "source" face (center face in the illustration in Fig. 1B), was morphed into an array of 12 different faces. The morphing level was either at 33% (1/3 morph) or at 67% (2/3 morph) of the full distance to the different-face condition. Subjects' task was to report whether a face image was identical or different from the previous face via a 2-button forced-choice response box. To give an objective measure for face similarities, the average Euclidean distance (see Methods) of the face stimuli in the different condition was 25.62. However, note that slight shifts in image position were introduced in all conditions between consecutive images to equalize for Euclidean distance across conditions and to avoid motion cue confounds (see Methods for details).

Comparing all face blocks with the no stimulus condition revealed a widespread and highly significant fMRI activation in the visual cortex, extending to frontal cortex areas. The activation maps are depicted in Supplementary Figure 2. The overall pattern of activation was highly consistent both in the multisubjects analysis ($n = 12$, $P < 0.003$, RE, uncorrected, Supplementary Fig. 2A) and for single subjects (e.g., in Supplementary Fig. 2B).

Searching for regions within these activated areas, which showed a highly significant adaptation effect (i.e., higher activation to the different face condition compared with the identical condition), revealed a more focused activation map, which was centered on occipitotemporal cortex, with a gradual growth of adaptation from intermediate visual areas to high-order ones and was more prominent in the right hemisphere. Figure 2 depicts the regions showing the highest face adaptation effect ($n = 12$, $P < 0.003$, RE, uncorrected, presented on the same cortical maps as Supplementary Fig. 2A).

FFA Tuning Sensitivity: Block Design

To obtain a more quantitative analysis of the adaptation effect in face-related areas, we have chosen to define the ROI through internal localizer procedure (see Methods). This procedure allowed us to restrict the analysis to voxels that exhibit an adaptation profile in the FFA cortex outside retinotopic areas (see Table 1 for more anatomical details of the ROIs).

The activity levels and response profiles obtained from the fusiform activations are depicted in Figure 3 (top, A,B—activation levels, bottom, C,D—response profiles). The localizer results are displayed on the left (Fig. 3A,C) as a reference to indicate that the analyzed data are consistent (see Table 2, Test 1 for verification of the statistical significance of this consistency). On the right of Figure 3(B,D) are the results from the independent measurements, which the following analysis elaborates on.

We found a clear adaptation effect (BOLD PSC: identical 0.62 ± 0.16 , different 1.33 ± 0.24). The critical result, however, is

in the activation levels of the 1/3 morph condition. Note that amplitude similar to the identical condition would mean no sub-exemplar sensitivity, whereas activation similar to the different condition (release from adaptation) would mean high sub-exemplar sensitivity. The results show a full release from

adaptation during the 1/3 morph condition (PSC—identical: 0.62 ± 0.16 , 1/3 morph: 1.16 ± 0.20 , 2/3 morph: 1.12 ± 0.18 , different: 1.33 ± 0.24) with amplitude not significantly lower than the different condition's amplitude. A statistical analysis of this data confirms this finding (see Table 2, Tests 2 and 3).

Table 2
Summary of ANOVA results

Test number	Data set	<i>n</i>	Purpose	Experiment	Factors	Effect	Interaction	Post hoc (Bonferroni/Dunn) contrast, <i>P</i>
1	FFA Internal localizer, combined (L + R)	10	Consistency between localizer and independent data	Block	Bias: localizer versus independent Condition: different versus identical	$F < 1$, $P > 0.84$ $F > 26$, $P < 0.0007$	$F < 1$, $P > 0.7$	
2	FFA internal localizer (independent data), only subjects with L and R foci	7	L versus R? when is release from adaptation	Block	Hemisphere	$F = 2.75$, $P > 0.14$		
					Condition (block)	$F > 11$, $P < 0.0003$	$F = 1.56$, $P > 0.23$	Identical – 1/3 morph , $P < 0.0008$ 1/3 morph – 2/3 morph, $P > 0.94$ 1/3 morph – different, $P > 0.11$
3	FFA internal localizer (independent data), combined (L + R)	10	When is release from adaptation	Block	Condition (block)	$F > 22$, $P < 0.0001$		Identical – 1/3 morph , $P < 0.0001$ 1/3 morph – 2/3 morph, $P > 0.67$ 1/3 morph – different, $P > 0.07$
4	FFA, faces > fixation (beyond retinotopy) combined (L + R)	11	Verification of test number 3: samples all FFA population; L versus R	Block	Hemisphere	$F = 0.84$, $P > 0.38$		
					Condition (block)	$F > 10.5$, $P < 0.0001$	$F = 2.28$, $P > 0.10$	Identical – 1/3 morph , $P < 0.007$ 1/3 morph – 2/3 morph, $P > 0.39$ 1/3 morph – different, $P < 0.017^*$ Identical – 1/3 morph, $P = 0.0381$ Identical – 2/3 morph, $P = 0.0174^*$
5	OFA internal localizer, combined (R + L)	6	When is release from adaptation	Block	Condition (block)	$F > 6.6$, $P < 0.005$		Identical – different , $P < 0.0006$ Identical – 10% morph, $P > 0.87$ 10% morph – 30% morph , $P < 0.005$ 30% morph – 40% morph, $P > 0.82$
6	FFA (R) 40% morph > identical	6	When is release from adaptation	Event related	Condition (event related)	$F > 8.4$, $P < 0.002$		
7	FFA faces > fixation (beyond retinotopy), only with both L + R foci	6	L versus R; verification of test number 6: sample all FFA population	Event related	Hemisphere	$F = 2.47$, $P > 0.17$		
					Condition (event related)	$F > 9.08$, $P < 0.002$	$F = 1.51$, $P > 0.25$	Identical – 10% morph, $P > 0.99$ 10% morph – 30% morph , $P < 0.008$ 30% morph – 40% morph, $P > 0.87$
8	OFA 40% morph > identical combined R + L	5	When is release from adaptation	Event related	Condition (event related)	$F > 7.6$, $P < 0.005$		Identical – 10% morph, $P > 0.80$ 10% morph – 30% morph, $P = 0.032^*$ 10% morph – 40% morph , $P < 0.003$
9	RT of subjects with FFA adaptation	6	Behavior as confound	Behavior (event related)	Condition (event related)	$F > 3.8$, $P < 0.04$		10% morph – 40% morph , $P < 0.005$ 10% morph – 30% morph, $P > 0.12$
10	RT of all subjects	8	Behavior as confound	Behavior (event related)	Condition (event related)	$F > 6.6$, $P < 0.003$		10% morph – 40% morph , $P < 0.0003$ 10% morph – 30% morph, $P > 0.11^*$

Note: Condition (block): identical, 1/3 morph, 2/3 morph, different; condition (event related): identical, 10% morph, 30% morph, 40% morph; Hemisphere: left and right; Significant effects are indicated in bold.

*significant only for *P* (corrected for multiple comparisons) ≤ 0.0083 .

To rule out a possibility that this activation profile resembles the activity in a subpopulation of the FFA cortex or that we bias the results by sampling the data according to a partial adaptation profile, we then verified our results via an additional analysis. We sampled all voxels in FFA cortex that showed activation to faces over the fixation baseline ($n = 11$, see Methods for details and Table 1 for anatomical details). The results of this analysis are provided in Supplementary Figure 3. A statistical analysis revealed the same results as the internal localizer analysis (Table 2, Test 4). So although we sample the data here without adaptation constraints, taking into account all face-activated voxels in FFA cortex, we still get a very significant release from adaptation in the 1/3 morph condition.

Thus, because we found strong recovery from adaptation in the 1/3 morph condition, the results clearly support the sub-exemplar tuning principle in the FFA.

OFA Tuning Sensitivity: Block Design

Although an adaptation focus in the right OFA region was clearly noticeable in the multisubject analysis (Fig. 2), when examining the adaptation levels in single subjects, we found that only 6 (out of the 12 subjects) exhibited significant adaptation foci in OFA (see Table 1 for more anatomical details of the ROIs). This might be due to the greater sensitivity to translation that was found in this region (Grill-Spector and others 1999) and that was imposed in each block in the experiment (controlled and counterbalanced, see Methods).

We now examined the adaptation profile of these OFA foci, as done in the FFA, using the internal localizer approach (Supplementary Figs 1 and 4). Although the FFA exhibited clear sub-exemplar tuning, the same analysis in OFA revealed an intermediate profile. When we examine the independent BOLD measurements (PSC—identical: 1.18 ± 0.38 , 1/3 morph: 1.65 ± 0.22 , 2/3 morph: 1.62 ± 0.28 , different: 2.06 ± 0.38), we found an effect for condition (analysis of variance[ANOVA]: $F > 6.6$, $P < 0.005$, for more details see Table 2, Test 5). But, although there was a trend for an enhancement of the signal (release from adaptation) in the 1/3 morph condition, it did not reach significance, likely due to the more variable adaptation effect in this region.

Measuring Face Tuning: Event Related

The block design approach allowed us to bracket the sensitivity of face changes to about 30% morph (especially in the FFA). In order to obtain a more precise delineation of this sensitivity as well as remove expectation and global attentional effects, we have approached the face-tuning adaptation question using a rapid event-related paradigm (Kourtzi and Kanwisher 2001).

Behavioral Experiment and Results: Event Related

To determine the parameters that will be used in the fMRI scans, we first ran a psychophysical test on 7 naive subjects that did not participate in the fMRI experiments. The results are summarized in Figure 4. The perceived difference is shown as a function of the amount of morph imposed on the stimuli. As can be seen, perceiving a difference starts at morph levels of 20% and reaches a plateau (of >90% performance) at 40% morph.

Following these results, we decided to include in the rapid event-related fMRI experiment 4 main conditions: identical, 10% morph (still below difference-perception), 30% morph, and

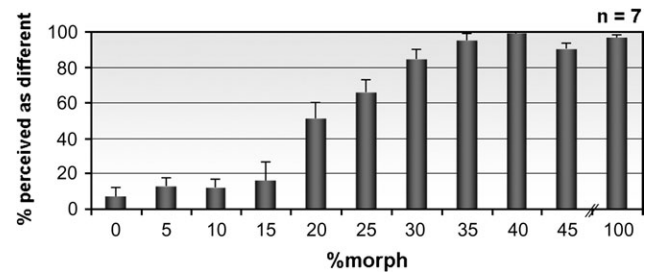


Figure 4. When do we perceive a face difference?—Behavioral results. Detection of face difference in 7 naive subjects as a function of the level of morphing imposed on the stimuli. Eleven morph levels (x axis) and fixation were tested (see Methods for details). The y axis represents the percentage of responses that “noticed a difference” out of all the responses. Error bars indicate standard error of mean. It is clear that subjects began noticing a difference at about 20% morph, and at 40% morph, difference was already fully recognized.

40% morph (the latter two bracketing the 1/3 morph condition from the block design experiment), and a fixation condition, all randomly interleaved. Events lasted 3000 ms consisting of visual presentation of 1200 ms followed by 1800-ms fixation screen (for experimental design, see Supplementary Fig. 5). Each visual presentation consisted of 4 rapid flashes of faces (200 ms face, 100 ms fixation), although the subject’s task was to report whether or not any difference was noticed among the faces.

FFA Face Tuning: Event Related

To localize the relevant voxels that show adaptation to faces, we first mapped the voxels showing preferential activation to the 40% morph compared with the identical-face condition. The left hemisphere showed no consistent adaptation and therefore was not included in this analysis. The analysis was based on 6 (out of 8) subjects who showed consistent adaptation in the right FFA (Table 1 specifies ROI anatomical details). Figure 5 depicts the activations in these regions to the various morph conditions. Note that the significant change in adaptation level occurred when moving from 10% morph to 30% morph. This was verified via a 1-way ANOVA (see Table 2, Test 6 for more details) and can be seen clearly both in the peak activation (Fig. 5A, 6 s after stimulus onset) and in the hemodynamic response function (HRF) of each condition (Fig. 5B), where the HRF of the 10% morph was similar to that of the identical condition, whereas the 30% morph matched the HRF of the 40% morph.

As in the block design analysis, here too, we also sampled all voxels in FFA that showed activation to faces over fixation baseline ($n = 8$, see Methods for details), to rule out possible sampling confounds (see Table 1 for ROI description). The results of this analysis support the results obtained from voxels showing preferential activation to 40% morph over identical and can be seen in Supplementary Figure 6. A statistical analysis verified the results (see Table 2, Test 7).

OFA Tuning: Event Related

Following the same analysis done in the FFA in the event-related experiment, 5 (out of the 8) subjects showed consistent adaptation in the OFA beyond retinotopic areas (4—both hemispheres, 1—right only, see Table 1). Further analysis of the data revealed a step in activation between the 10% morph and the 40% morph condition, as compared with the 10%

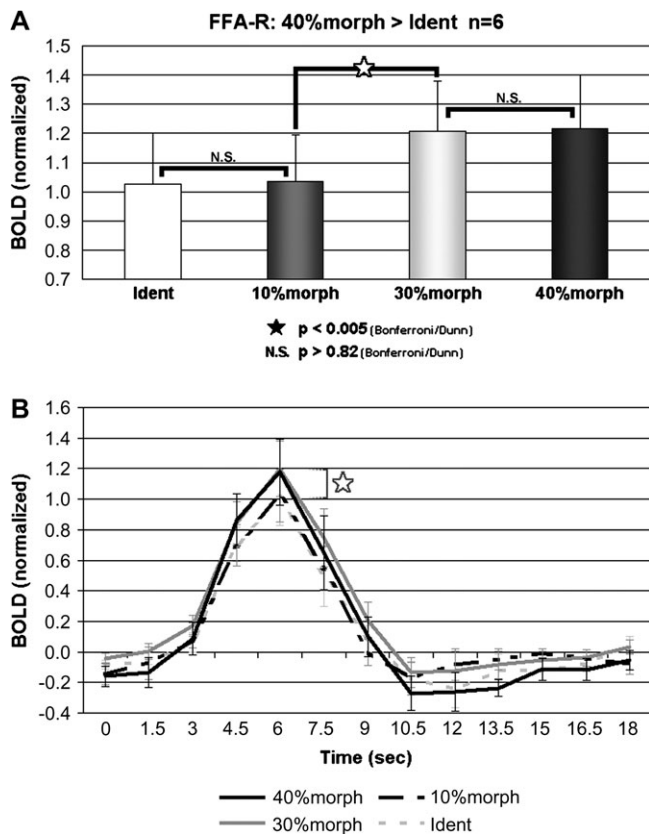


Figure 5. Right FFA activation during event-related face adaptation experiment. Average activation levels of the right FFA from 6 subjects that were significantly activated to the 40% morph > identical contrast (left FFA did not show consistent adaptation), in the 4 different conditions. (A) Histogram based on the maximal activation level of the HRF. (B) The HRF of these same voxels. A significant recovery from adaptation can be seen when moving from 10% morph to 30% morph, where the 10% morph activation profile almost replicates the identical condition and the 30% morph tightly follows the 40% morph. *P* values indicate 1-way ANOVA (for condition) post hoc Bonferroni/Dunn test results. Error bars indicate standard error of mean.

morph to 30% morph step found in the FFA (for specific details, see Table 2, Test 8). This again indicates that the sensitivity of the OFA does not reach the sub-exemplar level, which we do find in the FFA. However, additional work needs to fully confirm this.

The Possible Role of Task Difficulty and Attentional Load

It may be argued that the increased activation in the sub-exemplar morphing conditions (e.g., 30% morph) might be due to task difficulty or attentional load effects. Thus, it could be that the sub-exemplar changes in these conditions made it more difficult and attention consuming to perform the task compared with the identical condition, causing the enhanced activation we observed. We addressed this issue by examining whether changes in reaction time could have explained the variance in activation level in the fusiform voxels that we sampled. A pairwise correlation between the average BOLD activation levels and average RT was calculated to examine this. For the 6 subjects with right FFA foci to the contrast 40% morph > identical (corresponding to the data presented in Fig. 5), the correlation was $R^2 = 0.011$. The same analysis for the FFA data (right and left, $n = 8$) that was sampled by the contrast faces > fixation (matching data presented in Supplementary Fig. 6) yielded $R^2 = 0.008$. Clearly, no correlation can be discerned

between the normalized BOLD signal in the FFA and RT. To examine the possibility that there was a within-subject effect of difficulty that may explain the fMRI results, we ran an ANOVA on the RT (see Table 2, Tests 9 and 10). This analysis revealed a significant difference for the RT of the 10% morph versus 40% morph, but no significant difference was observed between the RT of the 10% morph versus the 30% morph. Note that this result argues against a role for RT in explaining the BOLD activation levels in the right FFA because we found a clear and significant release from adaptation even in the 30% morph level, with no corresponding difference in the RT. Thus, it is very unlikely that the results could be explained by task difficulty or attentional load effects.

Relationship of FFA's Release from Adaptation to Behavioral Performance

Having found high sensitivity for sub-exemplar changes in the FFA, it was of interest to examine to what extent the recovery from adaptation correlated with the behavioral face sensitivity. Thus, we wanted to quantitatively compare the relationship between the fMRI data and the behavioral performance. Because the effect we were looking for (relation between fMRI-adaptation and behavior) is specific to regions that undergo adaptation, we have chosen to base this analysis on the voxels that exhibit adaptation (using the internal localizer approach). To that end, we calculated adaptation recovery factor for the block design and event-related experiments and superimposed it on the behavioral data obtained from the psychophysical measurements performed outside the magnet and the measured performance of subjects during the fMRI scan (Fig. 6, see Methods for details). Examination of these plots reveals an intriguing correlation between the fMRI release from adaptation and the behavioral face sensitivity of the subjects.

Discussion

Sub-exemplar Tuning of the Adaptation Effects

Using 2 different experimental paradigms, we show that even levels of face changes at the sub-exemplar level, which were below the 50% perceptual exemplar (identity) boundary (Beale and Keil 1995; Campanella and others 2000), were sufficient to produce a complete recovery from adaptation in high-order face-related cortex, especially in the FFA (Kanwisher and others 1998). Thus, 30% morphing of faces was sufficient to produce activation levels that were not significantly different from activations to completely different faces. Thus, our results support a model of sub-exemplar tuned neuronal profiles in which facial changes within the perceptual exemplar boundary are sufficient to move the activation from one population of neurons to another.

The results cannot be explained by task difficulty or attentional effects, because when correlating them with RTs—which are an indication to task difficulty and attentional load—no correlation was observed between activity and this parameter in these areas. Also, arousal and expectation cannot serve as an explanation because the results of the block design were replicated in a randomly interleaved event-related paradigm in which such effects should be minimized.

How do our results fit with single-unit recordings, currently available from studies in inferotemporal cortex of the monkey? Face-responsive neurons were spotted in various aspects of monkey temporal cortex (Desimone and others 1984; Baylis

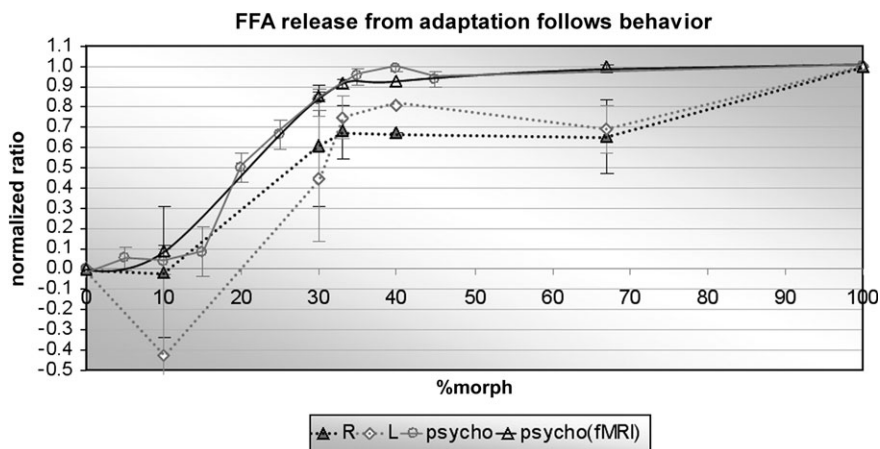


Figure 6. Relationship of fMRI data and behavioral performance. FFA release from adaptation (normalized adaptation ratios, block design, $n = 10$, event-related experiment, $n = 6$, see Methods) and behavioral sensitivity to face changes (behavioral experiment, $n = 7$, fMRI subjects' behavior [$n = 16$ as detailed above]) plotted together after data scaled to normalized units (for details see Methods). Gray circles, behavioral experiment; black open triangles, fMRI subjects' behavior; black filled triangles, right FFA; gray diamonds, left FFA. x axis denotes amounts of morphs (0, identical; 100, different). Error bars, standard error of mean. Note how the right FFA's release from adaptation follows nicely the behavioral gradient, where at morph levels $\leq 30\%$ there was already a significant release from adaptation, implying a direct link between neuronal tuning and behavioral sensitivity.

and others 1987; Yamane and others 1988; Gross 1992; Perrett and others 1992; Rolls 1992; Young and Yamane 1992; Sugase and others 1999). It seems that a portion of these face-responsive neurons are also primarily responsive to faces, that is, face selective. Within cortical regions that have face-selective neurons, there seems to be subpartitioning of populations, where the ventral aspect of inferotemporal cortex (also referred to as inferior temporal gyrus [ITG]) is mainly occupied with the identity and recognition aspects of face processing and seems to resemble the human FFA and OFA, whereas the human superior temporal sulcus (STS) face-selective area is a probable homologue of the monkey aSTS, dealing with facial expression, gesture, and movement. The portion of face-selective neurons in the ITG monkey cortex varies among studies and is in the range of 4–10% (e.g., 5% [Yamane and others 1988; Young and Yamane 1992], 8% [Sugase and others 1999]). Despite the limited stimulus set that single-unit studies can employ and their limited cortical coverage, various studies report on differential activation to different faces regardless of their facial expression (Baylis and others 1985; Hasselmo and others 1989; Rolls 1992). The hypothesis that arises from these studies is that facial representation is based on an ensemble or population coding (Baylis and others 1985; Gross 1992; Rolls 1992; Young and Yamane 1992), sparse or distributed.

The extent of activation we found in the current study, as well as other fMRI studies (Grill-Spector 2003; Levy and others 2004b), suggests that the neuronal representation underlying face-recognition is based on population coding. The sub-exemplar tuning width that we find with fMR-adaptation matches nicely the differential responses of single face-selective neurons to different faces, as was reported in single-unit studies (Baylis and others 1985; Hasselmo and others 1989; Rolls 1992). The results presented here are therefore compatible with these single-unit results from macaque inferotemporal cortex, where changes in the facial stimuli resulted in a marked change in the neuronal activity.

When examining fMRI studies regarding the aspect of face tuning, Pourtois and others (2005) showed view-sensitive repetition effects in face-selective regions to unfamiliar faces,

using rapid event-related paradigm. This view dependency could also be considered as support for sub-exemplar tuning within identity in face-selective regions. A recent study by Loffler and others (2005) has also employed fMR-adaptation to examine face tuning in face-selective cortex. Based on their results, they suggest that an important component in face coding could be the identity rather than face distinctiveness (distance). This resembles our finding that once the FFA is sensitive to a change in the stimulus it is less important “how much” of that change exists (resembling in our case the amount of morph, and our result that the recovery from adaptation for the 1/3 morph is already complete). And when we relate to the axes being examined, their direction condition resembles our parametric morph axis, whereas their distance condition resembles Rotshtein's morph axis (Rotshtein and others 2004), which could also account for the differences in the sensitivities reported in these studies. So although their experimental design varies from ours in many aspects (e.g., stimuli, task), and although their study does not relate to the behavioral and perceptual aspects, as well as to the correlation between the recorded signal and behavioral measures, it seems that their results are very much in line with ours, regarding the sensitivity profile of the FFA. Other studies examining cortical coding properties of faces have also used fMR-adaptation (repetition suppression) (Rotshtein and others 2001; Henson and others 2002; Ishai and others 2004; Winston and others 2004; Mazard and others 2005), but because various facial aspects (such as familiarity, expressions, emotional valence of the stimuli, orientation) were varied in these experiments and they might play a major role in facial coding systems in the cortex, we cannot directly relate our results to theirs.

Correlation of Behavioral Tuning and FFA Neuronal Tuning

The sensitivity we find in the FFA (through the release from adaptation effect) was at the sub-exemplar level (30% morph), significantly below the exemplar boundary (at 50% morph). Interestingly, this tuning paralleled the psychophysical performance of subjects (Figs 4 and 6) that was reflected in their

ability to detect face changes in rapid presentation. Assuming that the adaptation effect reflects the activity of neuronal groups, these results suggest that the behavioral tuning of subjects, reflected in their ability to detect subtle face changes, could be directly traced down to the tuning properties of the neuronal populations that were involved in the representation of these faces.

The fact that the magnitudes of fMR-adaptation to faces with near threshold differences in appearance parallel psychophysical measures of the detectability of those differences suggests that fMR-adaptation, as measured at the coarse level of fMRI, is closely related to behavior and to the information that can be read out of population responses.

Right and Left FFA Differences

There have been several studies pointing to a laterality difference between the right and left FFA, based both on reported clinical cases (Sergent and Villemure 1989; De Renzi and others 1994; De Renzi 1997) and on functional studies (Sergent and others 1992; Kanwisher and others 1997). Here, we found a tendency for the right FFA to be more consistently adapted than the left FFA. First, in the multisubject adaptation map of the block design experiment (Fig. 2), the adaptation extent of the right hemisphere was greater than that of the left hemisphere, at any given threshold. Also, we found more significant adaptation foci in the right hemisphere than in the left hemisphere (7 vs. 10 in the block design [out of 12] by the internal localizer procedure and 5 vs. 6 in event related design [out of 8]). This tendency, however, did not reach statistical significance. When we examined face-activated foci (defined by faces > fixation contrast) in the block design experiment, 11 subjects exhibited bilateral FFA activation foci, and a statistical analysis did not indicate a laterality difference in the activation profile ($P < 0.38$). This is also apparent when examining the event-related experiment data with face > fixation contrast. Here we found an equal number of foci bilaterally (6 subjects with bilateral foci, 1 with left-only focus, 1 with right-only focus) with no apparent laterality difference in the activation profile ($P < 0.175$). Concerning the selectivity profile, it appears that on average the right FFA showed a higher sensitivity curve (with a full recovery from adaptation at morph levels of 10–30%) compared with a more less sensitive left hemisphere (30% or higher), but again, this is not significant. So our results do not point to a clear distinction regarding the adaptation profile and the sensitivity of the neuronal population between the 2 hemispheres.

Adaptation Localized to Occipitotemporal Cortex

Although the most parsimonious interpretation of the results is that they reflect the sensitivity profile of individual neurons, we cannot rule out at this point that a more complex mechanism—such as adaptation at dendritic inputs or some network interactions—may be responsible for the fine tuning of the adaptation effect. It could also be argued that the adaptation effects are merely a reflection of feedback activity originating in, for example, frontal cortex regions. However, as can be seen in Figure 2, the main adaptation effects could be found only in occipitotemporal cortex and were absent in prefrontal regions. This was confirmed by time course analysis of prefrontal, as well as other, face-activated regions (not shown). It is interesting that a recent study (Ishai and others 2004) found fMR-adaptation in frontal cortex, as well as in posterior face-

selective regions. This discrepancy might be due to the different experimental paradigms that were employed in the different studies that might activate different neuronal mechanisms. Although in our study we used only neutral faces as experimental stimuli, Ishai and others (2004) used neutral and fearful faces. However, maybe a more prominent difference between the studies is due to the task. Here subjects were asked to detect differences between faces, whereas Ishai and others (2004) employed a memory oddball task. Oddball-related activation was reported earlier in the literature in prefrontal cortex (for partial overview, see Huettel and McCarthy 2004). So it might be that the basic neuronal mechanism of detecting face differences resides in the posterior lateral-occipital part of the brain and additional neuronal mechanisms that handle memory aspects are joining in when required (Ishai and others 2004). A different paper (Winston and others 2004) exploiting fMR-adaptation with faces examined the presumable dissociation between 2 face-processing streams—a ventral one for coding identity and a more rostral STS region coding expression. They report on face-repetition suppression in the FFA and in the right STS for identity; however, they found that only in the STS region this effect was somewhat influenced by an expression-repetition effect. This is an additional support to the idea that other brain areas showing fMR-adaptation for faces are involved in other aspects of facial processing, apart from processing mere facial differences (e.g., expressions, emotional valence, social interactions, direction of gaze, gender-related processing). Henson and others (2002) examined different aspects of processing with fMRI facial repetition effects, and although their design and experiment varied considerably from ours, they find repetition suppression confined to the occipitotemporal cortex, with repetition enhancement (“anti-adaptation”) in parietal and frontal cortices. Andrews and Ewbank (2004) examined different aspects of facial processing in the visual system using fMR-adaptation and found adaptation only in the FFA face-selective area. STS face-selective area, on the other hand, did not exhibit any significant reduction in the signal for a repeated presentation of the same face but did show an enhancement of the signal for various viewpoints and expressions of the same face. These data seem to point to the possibility that the occipitotemporal cortex, specializing in face processing, is the dominant player in distinguishing between faces, either across individuals or across the many appearances of the same face.

FFA versus OFA

Differences between the functional profiles of the FFA and OFA were reported earlier in the literature—with FFA being more invariant to facial manipulations, such as translation, illumination, and rotation, and OFA more sensitive to retinotopic parameters (Grill-Spector and others 1999; Levy and others 2001). Other studies showed that the FFA and OFA also differ in their selectivity to faces over other object categories (Levy and others 2001; Andrews and Ewbank 2004; Grill-Spector and others 2004) and in other functional aspects (Haxby and others 2000; Andrews and Ewbank 2004; Rotshtein and others 2004). Here we also found that the adaptation was somewhat less consistent across subjects in OFA (6 vs. 10 subjects with significant foci in OFA vs. FFA, block experiment), and the extent of the adaptation was weaker in OFA (adaptation ratios—LO-face: 0.58 ± 0.11 , FFA: 0.45 ± 0.10 , block experiment). This does not, however, seem to be due to the average number of voxels included in the analysis because we found

the average cluster size in OFA greater than in the FFA (see Table 1). Because image translations were applied to all blocks (in a controlled and counterbalanced manner, see Methods) and the OFA parallels anatomically to LO region, which is sensitive to this manipulation (Grill-Spector and others 1999), this might serve as a partial explanation. The profile of recovery from adaptation, as revealed in the block and the event-related experiments, was also different. Although in the right FFA we saw a clear step of activation in the block data between the 0% and 33% morph (1/3 morph condition), in OFA we did not observe such a clear step of activation and the change was more gradual in the block data, indicating less sensitivity to changes in the sub-exemplar level. Additional future work will have to be done in order to clearly define the OFA facial tuning width and check whether it really is less sensitive than the FFA's, as our results indicate. These results support earlier propositions that OFA may be less specific to face processing compared with the FFA.

Sub-exemplar Sensitivity to Unfamiliar Faces

An intriguing issue concerns the fact that the faces presented were unfamiliar to the subjects. This suggests that prior to the exposure to these faces, the neuronal circuitry in the FFA was already sensitive at the sub-exemplar level—although the subjects had never seen these specific exemplars of faces before. Interestingly, the recent report using famous faces (Rotshtein and others 2004) suggests that familiarizing with the faces actually appears to broaden the selectivity in the FFA and that no release from adaptation is observed for a 30% level of morph—when within identity (sub-exemplar, not crossing the 50% morph exemplar boundary). They find release from adaptation with this level of morph only when crossing the 50% morph exemplar boundary (between identity). They conclude that the right FFA is mainly sensitive to identity and not to the physical aspects of a face. Here, we show complementary results for unfamiliar faces, where the right FFA is sensitive to much subtler changes within identity (sub-exemplar changes). Our results, together with those reported by Rotshtein and others (2004), support the possibility that the neuronal representation changes as a function of the familiarity. This is in line with previous findings suggesting that there are differences both in the behavioral aspect and in the neuronal representation between famous and unfamiliar faces (Beale and Keil 1995; George and others 1999; Hancock and others 2000).

At this point, we can only speculate as to the source of such high selectivity to unfamiliar faces. One possibility is a very rapid tuning effect—by which after only few initial exposures the system already becomes “familiar” with the faces and develops high selectivity to them. This possibility may seem counterintuitive, but it should be noted that behaviorally, unfamiliar face images can be remembered following a single exposure (Bruce and others 1991). Also, adaptation effects occur very rapidly, even upon a second presentation of an image (Kourtzi and Kanwisher 2001). Alternatively, it could be that the memory capacity of the system is very large (Levy and others 2004b), so that the “library” of face images already contained within it is sufficient to allow the sub-exemplar sensitivity observed even to unfamiliar faces. Another possibility is that many of the neurons are not tuned to full faces but rather to intermediately complex fragments (Ullman and others 2002) that are not unique to familiar faces.

It should also be noted that although the sensitivity we find is in the sub-exemplar level, it is not absolute. Thus, 10% morphing failed to cause adaptation release. Hence, such width of tuning might allow the system sufficient flexibility to accommodate and be modified by new, unfamiliar faces (Poggio and Bizzi 2004). More modeling and experimental results will be needed to resolve this issue.

Possible Implications of the Results to the Face-Tuning Properties of Cortical Neurons

Considering the present results in the context of previous fMRI studies of the human face and object areas leads to an apparent paradox. The problem lies in that the activity associated with each face image is likely to involve millions of neurons—this can be qualitatively deduced simply from the fact that a measurable fMRI signal is generated in event-related studies. Recently, we (Levy and others 2004b) have derived such conclusion from more quantitative considerations. On the other hand, the present results illustrate that the neuronal population is highly tuned to each face template. Putting these findings together and considering that the human visual system is undoubtedly capable of recognizing many thousands (Landauer 1986), and likely even millions of different faces and object images, it appears that there are simply not enough cortical neurons available to represent such vast library of images. Three possible outcomes could be suggested for this dilemma. First, that each neuron may represent only a tiny fragment or a small feature from the face image (Fujita and others 1992), and hence, there is a highly distributed activation produced by each face (which includes many such fragments). However, this possibility is not supported by recent fMRI results that point to a rather “holistic” nature of the neuronal response—in which the neurons are sensitive to the entire or at least large part of the face or object image template (Hasson and others 2001; Kourtzi and Kanwisher 2001; Lerner and others 2001, 2002, 2004). The second possibility is that the neurons are broadly tuned, so each neuron responds in a highly redundant level to many faces. This possibility is ruled out by the present results that demonstrate high selectivity at the sub-exemplar level. The only alternative that remains is that each neuron in the face-related areas is sensitive to many (perhaps millions of) different face (or even object) templates in a sharply tuned manner. In such a model the “receptive field” of each neuron is essentially an “or” function of a whole library of different templates. However, the tuning to each of these templates is highly selective. Importantly, under this scheme, the library of templates that activate each neuron is different. Thus, different face images will elicit different patterns of responses in the entire neuronal population. A unique face representation can then be obtained through the group response profile.

Although not discussed explicitly in the neurophysiology literature, such a model is compatible with a surprising ease by which a very limited library of images that are used in typical single-unit recording sessions (often less than a hundred) in the human and monkey object areas elicit robust neuronal responses (e.g., Kreiman and others 2000; Freedman and others 2001, 2003).

Extension to Other Object Categories

To what extent are these results relevant to other object categories? Although the issue of whether faces are “special” is still debated, it appears that general principles of representation,

such as the various viewing invariances (Grill-Spector and others 1999) and holistic and completion effects (Hasson and others 2001; Kourtzi and Kanwisher 2001; Lerner and others 2002) are comparable. Of course, the difference between the representation of faces and the representation of general object categories might be precisely in the domain of shape-tuning selectivity. Thus, it may be that faces are special by virtue of the fact that the shape tuning of their neurons is narrower. We are currently examining this issue in more detail.

Supplementary Material

Supplementary material can be found at: <http://www.cercor.oxfordjournals.org/>.

Notes

This study was funded by the Israel Science Foundation Center of Excellence, the Benozio Center for Neurological Disorders, and the Dominique Center. We thank Ifat Levy, Kalanit Grill-Spector, Galia Avidan, and Yulia Golland for fruitful discussions during the study. We thank Ifat Levy, Yulia Golland, Roy Mukamel, and Yuval Nir for comments on the manuscript. We thank M. Harel for help with the brain-flattening procedure and E. Okon for technical assistance. We thank the Functional Brain Imaging (fMRI) Unit in the Wohl Institute of Advanced Imaging, Sourasky Medical Center, Tel Aviv. We thank the Computer Vision Laboratory, Faculty of Computer and Information Science, University of Ljubljana, Ljubljana, Slovenia, and the Secondary School Centre, Velenje, Slovenia, for allowing us to use the CVL Face Database (<http://www.lrv.fri.uni-lj.si/facedb.html>). *Conflict of Interest*: None declared.

Address correspondence to Prof. Rafael Malach, Department of Neurobiology, Weizmann Institute of Science, Rehovot 76100, Israel. Email: rafi.malach@weizmann.ac.il.

References

Andrews TJ, Ewbank MP. 2004. Distinct representations for facial identity and changeable aspects of faces in the human temporal lobe. *Neuroimage* 23:905-913.

Baylis GC, Rolls ET, Leonard CM. 1985. Selectivity between faces in the responses of a population of neurons in the cortex in the superior temporal sulcus of the monkey. *Brain Res* 342:91-102.

Baylis GC, Rolls ET, Leonard CM. 1987. Functional subdivisions of the temporal lobe neocortex. *J Neurosci* 7:330-342.

Beale JM, Keil FC. 1995. Categorical effects in the perception of faces. *Cognition* 57:217-239.

Beauchamp MS, Argall BD, Bodurka J, Duyn JH, Martin A. 2004. Unraveling multisensory integration: patchy organization within human STS multisensory cortex. *Nat Neurosci* 7:1190-1192.

Bruce V, Doyle T, Dench N, Burton M. 1991. Remembering facial configurations. *Cognition* 38:109-144.

Campanella S, Hanoteau C, Depy D, Rossion B, Bruyer R, Crommelinck M, Guerit JM. 2000. Right N170 modulation in a face discrimination task: an account for categorical perception of familiar faces. *Psychophysiology* 37:796-806.

De Renzi E. 1997. Prosopagnosia. In: Feinberg TE, Farah M, editors. *Behavioral neurology and neuropsychology*. New York: McGraw-Hill. p 245-256.

De Renzi E, Perani D, Carlesimo GA, Silveri MC, Fazio F. 1994. Prosopagnosia can be associated with damage confined to the right hemisphere—an MRI and PET study and a review of the literature. *Neuropsychologia* 32:893-902.

Desimone R, Albright TD, Gross CG, Bruce C. 1984. Stimulus-selective properties of inferior temporal neurons in the macaque. *J Neurosci* 4:2051-2062.

DeYoe EA, Carman GJ, Bandettini P, Glickman S, Wieser J, Cox R, Miller D, Neitz J. 1996. Mapping striate and extrastriate visual areas in human cerebral cortex. *Proc Natl Acad Sci USA* 93:2382-2386.

Engel SA, Glover GH, Wandell BA. 1997. Retinotopic organization in human visual cortex and the spatial precision of functional MRI. *Cereb Cortex* 7:181-192.

Freedman DJ, Riesenhuber M, Poggio T, Miller EK. 2001. Categorical representation of visual stimuli in the primate prefrontal cortex. *Science* 291:312-316.

Freedman DJ, Riesenhuber M, Poggio T, Miller EK. 2003. A comparison of primate prefrontal and inferior temporal cortices during visual categorization. *J Neurosci* 23:5235-5246.

Friston J, Holmes A, Worsley K, Poline J, Frith C, Frackowiak R. 1994. Statistical parametric maps in functional imaging: a general linear approach. *Hum Brain Mapp* 2:189-210.

Friston KJ, Holmes AP, Price CJ, Buchel C, Worsley KJ. 1999. Multi-subject fMRI studies and conjunction analyses. *Neuroimage* 10:385-396.

Fujita I, Tanaka K, Ito M, Cheng K. 1992. Columns for visual features of objects in monkey inferotemporal cortex. *Nature* 360:343-346.

Gauthier I, Skudlarski P, Gore JC, Anderson AW. 2000. Expertise for cars and birds recruits brain areas involved in face recognition. *Nat Neurosci* 3:191-197.

George N, Dolan RJ, Fink GR, Baylis GC, Russell C, Driver J. 1999. Contrast polarity and face recognition in the human fusiform gyrus. *Nat Neurosci* 2:574-580.

Gilaie-Dotan S, Malach R. 2004. High shape selectivity in human face-related areas. Program No. 258.9, 2004 Abstract Viewer/Itinerary Planner: San Diego, CA. Washington, DC: Society for Neuroscience.

Grill-Spector K. 2003. The neural basis of object perception. *Curr Opin Neurobiol* 13:159-166.

Grill-Spector K, Knouf N, Kanwisher N. 2004. The fusiform face area subserves face perception, not generic within-category identification. *Nat Neurosci* 7:555-562.

Grill-Spector K, Kushnir T, Edelman S, Avidan G, Itzhak Y, Malach R. 1999. Differential processing of objects under various viewing conditions in the human lateral occipital complex. *Neuron* 24:187-203.

Grill-Spector K, Kushnir T, Hendler T, Malach R. 2000. The dynamics of object-selective activation correlate with recognition performance in humans. *Nat Neurosci* 3:837-843.

Grill-Spector K, Malach R. 2001. fMR-adaptation: a tool for studying the functional properties of human cortical neurons. *Acta Psychol* 107:293-321.

Gross CG. 1992. Representation of visual stimuli in inferior temporal cortex. *Philos Trans R Soc Lond B Biol Sci* 335:3-10.

Halgren E, Dale AM, Sereno MI, Tootell RBH, Marinkovic K, Rosen BR. 1999. Location of human face-selective cortex with respect to retinotopic areas. *Hum Brain Mapp* 7:29-37.

Hancock PJ, Bruce VV, Burton AM. 2000. Recognition of unfamiliar faces. *Trends Cogn Sci* 4:330-337.

Hasselmo ME, Rolls ET, Baylis GC. 1989. The role of expression and identity in the face-selective responses of neurons in the temporal visual cortex of the monkey. *Behav Brain Res* 32:203-218.

Hasson U, Avidan G, Deouell LY, Bentin S, Malach R. 2003. Face-selective activation in a congenital prosopagnosic subject. *J Cogn Neurosci* 15:419-431.

Hasson U, Hendler T, Ben Bashat D, Malach R. 2001. Vase or face? A neural correlate of shape-selective grouping processes in the human brain. *J Cogn Neurosci* 13:744-753.

Hasson U, Nir Y, Levy I, Fuhrmann G, Malach R. 2004. Intersubject synchronization of cortical activity during natural vision. *Science* 303:1634-1640.

Haxby JV, Gobbini MI, Furey ML, Ishai A, Schouten JL, Pietrini P. 2001. Distributed and overlapping representations of faces and objects in ventral temporal cortex. *Science* 293:2425-2430.

Haxby JV, Hoffman EA, Gobbini MI. 2000. The distributed human neural system for face perception. *Trends Cogn Sci* 4:223-233.

Henson RN, Shallice T, Gorno-Tempini ML, Dolan RJ. 2002. Face repetition effects in implicit and explicit memory tests as measured by fMRI. *Cereb Cortex* 12:178-186.

Huettel SA, McCarthy G. 2004. What is odd in the oddball task? Prefrontal cortex is activated by dynamic changes in response strategy. *Neuropsychologia* 42:379-386.

Huk AC, Heeger DJ. 2002. Pattern-motion responses in human visual cortex. *Nat Neurosci* 5:72-75.

- Ishai A, Pessoa L, Bickle PC, Ungerleider LG. 2004. Repetition suppression of faces is modulated by emotion. *Proc Natl Acad Sci USA* 101:9827-9832.
- Ishai A, Ungerleider LG, Martin A, Schouten HL, Haxby JV. 1999. Distributed representation of objects in the human ventral visual pathway. *Proc Natl Acad Sci USA* 96:9379-9384.
- Kanwisher N, McDermott J, Chun MM. 1997. The fusiform face area: a module in human extrastriate cortex specialized for face perception. *J Neurosci* 17:4302-4311.
- Kanwisher N, Tong F, Nakayama K. 1998. The effect of face inversion on the human fusiform face area. *Cognition* 68:B1-B11.
- Kourtzi Z, Erb M, Grodd W, Bülthoff HH. 2003. Representation of the perceived 3-D object shape in the human lateral occipital complex. *Cereb Cortex* 13:911-920.
- Kourtzi Z, Kanwisher N. 2001. Representation of perceived object shape by the human lateral occipital complex. *Science* 293:1506-1509.
- Kreiman G, Koch C, Fried I. 2000. Category-specific visual responses of single neurons in the human medial temporal lobe. *Nat Neurosci* 3:946-953.
- Landauer TK. 1986. How much do people remember? Some estimates of the quantity of learned information in long-term memory. *Cognit Sci* 10:477-493.
- Le Grand R, Mondloch CJ, Maurer D, Brent HP. 2004. Impairment in holistic face processing following early visual deprivation. *Psychol Sci* 15:762-768.
- Leopold DA, O'Toole AJ, Vetter T, Blanz V. 2001. Prototype-referenced shape encoding revealed by high-level aftereffects. *Nat Neurosci* 4:89-94.
- Lerner Y, Harel M, Malach R. 2004. Rapid completion effects in human high-order visual areas. *Neuroimage* 21:516-526.
- Lerner Y, Hendler T, Ben-Bashat D, Harel M, Malach R. 2001. A hierarchical axis of object processing stages in the human visual cortex. *Cereb Cortex* 11:287-297.
- Lerner Y, Hendler T, Malach R. 2002. Object-completion effects in the human lateral occipital complex. *Cereb Cortex* 12:163-177.
- Levy I, Hasson U, Avidan G, Hendler T, Malach R. 2001. Center-periphery organization of human object areas. *Nat Neurosci* 4:533-539.
- Levy I, Hasson U, Harel M, Malach R. 2004a. Functional analysis of the periphery effect in human building related areas. *Hum Brain Mapp* 22:15-26.
- Levy I, Hasson U, Malach R. 2004b. One picture is worth at least a million neurons. *Curr Biol* 14:996-1001.
- Loffler G, Yourganov G, Wilkinson F, Wilson HR. 2005. fMRI evidence for the neural representation of faces. *Nat Neurosci* 8:1386-1390.
- Martinez A, Benavente R. 1998. The AR face database. CVC Technical Report nr 24 [database]. http://rv11.ecn.purdue.edu/~aleix/aleix_face_DB.html.
- Mazard A, Schiltz C, Rossion B. 2005. Recovery from adaptation to facial identity is larger for upright than inverted faces in the human occipito-temporal cortex. *Neuropsychologia*. Forthcoming.
- Mukamel R, Gelbard H, Arieli A, Hasson U, Fried I, Malach R. 2005. Coupling between neuronal firing, field potentials, and fMRI in human auditory cortex. *Science* 309:951-954.
- O'Toole AJ, Vetter T, Volz H, Salter EM. 1997. Three-dimensional caricatures of human heads: distinctiveness and the perception of facial age. *Perception* 26:719-732.
- Perrett DI, Hietanen JK, Oram MW, Benson PJ. 1992. Organization and functions of cells responsive to faces in the temporal cortex. *Philos Trans R Soc Lond B Biol Sci* 335:23-30.
- Poggio T, Bizzi E. 2004. Generalization in vision and motor control. *Nature* 431:768-774.
- Pourtois G, Schwartz S, Seghier ML, Lazeyras F, Vuilleumier P. 2005. Portraits or people? Distinct representations of face identity in the human visual cortex. *J Cogn Neurosci* 17:1043-1057.
- Rhodes G, Brennan S, Carey S. 1987. Identification and ratings of caricatures: implications for mental representations of faces. *Cognit Psychol* 19:473-497.
- Rhodes G, Carey S, Byatt G, Proffitt F. 1998. Coding spatial variations in faces and simple shapes: a test of two models. *Vision Res* 38:2307-2321.
- Rolls ET. 1992. Neurophysiological mechanisms underlying face processing within and beyond the temporal cortical visual areas. *Philos Trans R Soc Lond B Biol Sci* 335:11-20; discussion 20-11.
- Rotshtein P, Henson RN, Treves A, Driver J, Dolan RJ. 2004. Morphing Marilyn into Maggie dissociates physical and identity face representations in the brain. *Nat Neurosci* 8:107-113.
- Rotshtein P, Malach R, Hadar U, Graif M, Hendler T. 2001. Feeling or features: different sensitivity to emotion in high-order visual cortex and amygdala. *Neuron* 32:747-757.
- Sereno MI, Dale AM, Reppas JB, Kwong KK, Belliveau JW, Brady TJ, Rosen BR, Tootell RB. 1995. Borders of multiple visual areas in humans revealed by functional magnetic resonance imaging. *Science* 268:889-893.
- Sergent J, Ohta S, Macdonald B. 1992. Functional neuroanatomy of face and object processing. A positron emission tomography study. *Brain* 115:15-36.
- Sergent J, Villemure JG. 1989. Prosopagnosia in a right hemispherectomized patient. *Brain* 112(Pt 4):975-995.
- Spiridon M, Kanwisher N. 2002. How distributed is visual category information in human occipito-temporal cortex? An fMRI study. *Neuron* 35:1157-1165.
- Sugase Y, Yamane S, Ueno S, Kawano K. 1999. Global and fine information coded by single neurons in the temporal visual cortex. *Nature* 400:869-873.
- Talairach J, Tournoux P. 1988. Co-planar stereotaxic atlas of the human brain. New York: Thieme Medical Publishers.
- Tong F, Nakayama K, Moscovitch M, Weinrib O, Kanwisher N. 2000. Response properties of the human fusiform face area. *Cogn Neuro-psychol* 17:257-279.
- Tootell RBH, Reppas JB, Dale AM, Look RB, Sereno MI, Malach R, Brady TJ, Rosen BR. 1995. Visual-motion aftereffect in human cortical area MT revealed by functional magnetic-resonance-imaging. *Nature* 375:139-141.
- Ullman S, Vidal-Naquet M, Sali E. 2002. Visual features of intermediate complexity and their use in classification. *Nat Neurosci* 5: 682-687.
- Valentine T. 1991. A unified account of the effects of distinctiveness, inversion, and race in face recognition. *Q J Exp Psychol A* 43:161-204.
- Valentine T, Endo M. 1992. Towards an exemplar model of face processing: the effects of race and distinctiveness. *Q J Exp Psychol A* 44:671-703.
- Wilson HR, Loffler G, Wilkinson F. 2002. Synthetic faces, face cubes, and the geometry of face space. *Vision Res* 42:2909-2923.
- Winston JS, Henson RN, Fine-Goulden MR, Dolan RJ. 2004. fMRI-adaptation reveals dissociable neural representations of identity and expression in face perception. *J Neurophysiol* 92:1830-1839.
- Yamane S, Kaji S, Kawano K. 1988. What facial features activate face neurons in the inferotemporal cortex of the monkey? *Exp Brain Res* 73:209-214.
- Young MP, Yamane S. 1992. Sparse population coding of faces in the inferotemporal cortex. *Science* 256:1327-1331.